REGULAR ARTICLE

Charge transport and luminescent properties of $C_6F_5Cu(py)$ and their relationships with cuprophilic interactions: a density functional theory investigation

Fei Yu · Shui-Xing Wu · Yun Geng ·
Guo-Chun Yang · Zhong-Min Su

Abstract Weak interactions between copper atoms so called cuprophilic interactions, lead to the supramolecular stacks of $C_6F_5Cu(py)$, which possess unique luminescent and charge transport properties. First-principle band-structure calculations have been used to investigate the relationship between its charge transport property and cuprophilic interactions for the first time. The valence bandwidth was found three times larger than the conduction bandwidth. Meanwhile, the effective mass of hole is 0.46 m_0, which is only one-third of the electron, and much smaller than that of the pentacene. Thus, $C_6F_5Cu(py)$ would become a promising candidate for hole transport material. The analysis based on density of states and band structure shows that holes transport mainly along the direction of cuprophilic interactions (c-axis) and cuprophilic interactions are in favor of hole transport. Thus, the cuprophilic interactions play an important role in determining charge transport. By the replacement of copper atoms with silver and gold atoms, the results show that there are close relationships between the metallophilic interactions and transport ability, i.e., the stronger metallophilic interactions are, the better hole transport ability is. The solid state emission of $C_6F_5Cu(py)$ is attributed to the monomer rather than the dimer. This emission is assigned as the metal-to-ligand charge transfer (MLCT), and combined with some contributions from ligand-to-ligand charge transfer (LLCT).

Keywords $C_6F_5Cu(py)$ · Cuprophilic interactions · Band structure · Charge transport · DFT

F. Yu · S.-X. Wu · Y. Geng · G.-C. Yang (✉) · Z.-M. Su (✉)
Institute of Functional Material Chemistry,
Faculty of Chemistry, Northeast Normal University,
130024 Changchun, People's Republic of China
e-mail: yanggc468@nenu.edu.cn

Z.-M. Su
e-mail: zmsu@nenu.edu.cn

1 Introduction

Organic transport materials have been attracted a deal of attention for use in organic field-effect transistors (OFETs), solar cells, and organic light-emitting diodes (OLEDs), which possess great advantages such as low cost, easy fabrication, and mechanical flexibility [1–3]. The efficiency of these devices is determined by charge injection and transport, charge carrier balance, radiative decay of excitons, and light extraction. Especially, charge transport in organic materials is one of the most important factors in the performance of OLEDs [4, 5], organic field-effect transistors [6, 7], and organic solar cells [8, 9]. The continued emergence for these applications will mainly depend on performance enhancement in such materials.

In recent years, luminescent d^8 and d^{10} metal complexes have attracted much attention because of their potential applications in sensors and photochemical and electroluminescent devices [10–16]. These complexes show a wide range of luminescence properties that depend strongly on the structural and electronic characteristics of their ligands. Experimental [17–22] and theoretical [23–25] researches on these complexes indicate that metal–metal interaction also plays an important role in determining luminescence. Moreover, recent studies show that supramolecular organometallic nanostructures induced by metal–metal, C–H···π and hydrophobic interactions have exhibited excellent

electron- [26] and hole- [27] transporting abilities, which can be used as active components in miniature sensors, OFETs, and OLEDs. The metallophilic attraction is between metal atoms, or ions, with closed electron shells. The origin of this attraction arises primarily from weak dispersive effects and enhanced by relativistic effects in heavier element systems. They are weaker than most covalent or ionic bonds, but stronger than other van der Waals bonds, and roughly comparable in strength with typical hydrogen bonds [28–30]. Recently, lots of complexes containing weak d^{10}–d^{10} interactions have been reported [31–36]. The energy of Au(I)–Au(I) aurophilic interaction existing in the solid state and solution is estimated to be 30–60 kJ/mol [37–39] comparable to that of hydrogen bonds. Pyykkö and Mendizabal have attributed the aurophilic attraction to correlation effects, which are enhanced by relativistic effects.

Polynuclear d^{10} complexes have been obtained increasing attention in the past few years, due to their fascinating luminescent properties origining from their metal–metal and metal–ligand bonding natures, and they can be utilized as luminescent sensors [17, 40, 41], and LEDs [42, 43]. Omary et al. studied a series of polynuclear complexes of Cu(I) and Ag(I) with fluorinated pyrazolate ligand [44, 45]. Especially, {[3,5-$(CF_3)_2$Pz]Cu}$_3$ has the potential to use as emitting materials for molecular LEDs [42]. Furthermore, copper phthalocyanine (CuPc) is used as excellent hole transport material [46]. Yan et al. fabricated a series of organic heterojunction devices based on CuPc, exhibiting air stability and good ambipolar transport behavior [47]. Based on tetranuclear copper complex, Jakle et al. synthesized a series of organocopper complexes, through Cu-π, Cu–S, perfluoroarene–arene, and cuprophilic interactions. Some of these complexes possess fascinating luminescent properties [48, 49]. Treatment of pentafluorophenylcopper tetramer ($[C_6F_5Cu]_4$) with an equimolar amount of pyridine, a pale yellow dicoordinate organocopper complex ($C_6F_5Cu(py)$) was obtained, with a strong blue fluorescence band at 460 nm. The ligands in adjacent molecules are in a staggered conformation, which avoids any π-stacking interactions. And the copper atoms are arranged in one-dimensional chains with a distance of 2.892 Å, which is in the scope of metal–metal interaction [50]. This is the first time to form a supramolecular structure through cuprophilic interactions for dicoordinated organocopper complex.

With the development of quantum chemistry, especially in the photoelectric field, it is possible to explain the experimental phenomenon and design excellent photoelectric materials. For examples, Bredas et al. have used density functional theory (DFT) coupled with wide-band theory to discuss the impact of fluorine and alkyl/alkoxy substituents on oligoacene crystals and obtained a good

understanding of the role of substitution on the carrier-transporting process [51, 52]. Shuai et al. employed first-principle theory and deformation potential theory, calculated the size-dependent carrier mobility and its polarity in Graphene from band view, providing theoretical support to experimentalists for designing high-efficient charge transport materials [53]. Felice et al. carried out a comprehensive investigation of the structural and electronic properties of several isolated and periodic Pt2(dta)4I polymers using PBE exchange–correlation functional as implemented in the PWscf code. Their results show that the chain has a metallic behavior that is in agreement with the experimental findings at room temperature in the crystalline phase. The characteristics and the origin of the metallicity are deeply analyzed by changing the assembling of the constituent subunits of the original polymer in viable different ways [54]. Our group also investigated the charge transport mechanism of a series of organic photoelectric materials [55–57].

Due to its strong blue fluorescence emission, $C_6F_5Cu(py)$ can be used as a promising blue-emitting material. On the other band, thanks to the staggered formation of the ligands, the transporting properties could be tuned by the metal–metal interaction, and no theoretical study on the charge transport properties of complexes involving such interaction has been reported in the literature. Also, we can study the mechanism of the blue-emission on whether it is related to the metal–metal interaction. In this work, with the help of DFT calculations, dicoordinate organocopper complex $C_6F_5Cu(py)$ was taken as an example to study: (1) the relationship between the molecular-packing mode induced by the cuprophilic interactions and the charge transport, (2) insights on the excited states electronic structures and luminescent properties. Moreover, the influence of replacement of copper atom with silver and gold on the metal–metal interactions and charge transport is also investigated.

2 Theoretical methodology

Generally, there are two models to describe the charge transport mechanism at present: hopping model and band-like model. The charge transport is governed by hopping mechanism when the system is disordered at room temperature. But in the well-ordered organic crystals, the mobility is more rationally described by band-like model. Shuai et al. carried out first-principle band-structure calculations to the Tris(8-hydroxyquinolinato)aluminum (Alq$_3$) and concluded that Alq$_3$ is a good electron transport material from the band structure's view for the first time [58].

In a standard band-theory model, the group velocity $v(k)$ of the delocalized electron waves or hole waves is given by the gradient of the band energy in k-space,

$$\vec{v}(k) = \nabla_k E(k) \big/ \hbar \qquad (1)$$

where $E(k)$ is the band structure of the system, k the wave vector, and $\hbar = h/2\pi$, h is the Planck constant. Under the constant relaxation time approximation at low temperature, the mobility can be given by

$$\mu_\alpha = e\tau m_\alpha^{-1} \qquad (2)$$

Here, the inverse effective mass m_α^{-1} is a key parameter of the charge transport in the band-like model. The effective mass is related to the curvature of the minimum/maximum of the conductive band (CB)/valence band (VB). It reads

$$m_{\alpha\beta}^{-1} = -\frac{1}{\hbar^2} \left(\frac{\partial^2 E(k)}{\partial k_\alpha \partial k_\beta} \right) \qquad (3)$$

Here, subscripts α and β denote the Cartesian coordinates in reciprocal space, and $E(k)$ is the band energy. The heavier the effective mass is, the smaller the mobility is.

Density functional theory (DFT) [59, 60] calculations are carried out using Dmol^3 within the Material Studio package [61, 62]. It should be noted that there are certain limitations of current DFT functionals in accurately describing van der Waals forces in the molecular crystals. Byrd et al. have systemically tested the successes and failures of current DFT functionals and suggested that it is necessary to develop new DFT functionals which include accurate dispersion forces [63]. In this paper, the generalized gradient approximation (GGA) in the Perdew–Burke–Ernzerhof (PBE) [64] form and an all-electron double numerical basis set with polarized function (DNP basis set) are used to optimize the crystal structure, and the band structure, density of states, and also the Γ point wave function are calculated. The lattice parameter used here are $a = 9.891$ Å, $b = 18.948$ Å, $c = 5.785$ Å, and $\alpha = \beta = \gamma = 90°$. Integrations over the Brillouin zone were sampled by $10 \times 5 \times 10$ k points using the Monkhorst–Pack scheme. The binding energies of the dimers along c-axis are calculated under MP2 [65] level as implemented in the Gaussian 09 program [66]. The functional used in all is the Becke's exchange and Lee, Yang, and Parr's functional (B3LYP) [67, 68]. Basis sets of SDD [69, 70] containing relativistic effects were applied to metal (Cu, Ag, and Au) atoms and 6-31G** [71, 72] were applied to C, H, N, and F. The basis set superposition errors (BSSE) [73] was taken into consideration in binding energy calculations. Calculations on the excited state of the investigated complexes were carried out at the TDDFT/B3LYP level, using SDD basis set for metal atoms, and 6-31G** for other elements.

3 Results and discussion

3.1 Geometric structure

The monomer, crystal structure, and packing mode along c-axis of $C_6F_5Cu(py)$ are shown in Fig. 1. The crystal crystallizes in the orthorhombic space group $Pbcm$, with four molecules per unit cell. It exhibits a linear coordination geometry, with the pentafluorophenyl rings and the pyridine rings coplanar. The ligands in adjacent molecules are in a staggered formation, which can effectively avoid the π-stacking interactions. However, the arrangement of copper atoms in one-dimension chains leads to the supramolecular packing. The selected optimized bond lengths and bond angles along with experimental values are listed in Table 1. It can be seen that the calculated values are in good agreement with the experimental ones. The distance between copper atoms is 2.894 Å, which is only 0.002 Å different from the experimental value. This indicates that the adopted calculation method is suitable to the studied complexes. Such a short distance between copper atoms is close to the sum of the van der Waals radii of two Cu$^{\mathrm{I}}$
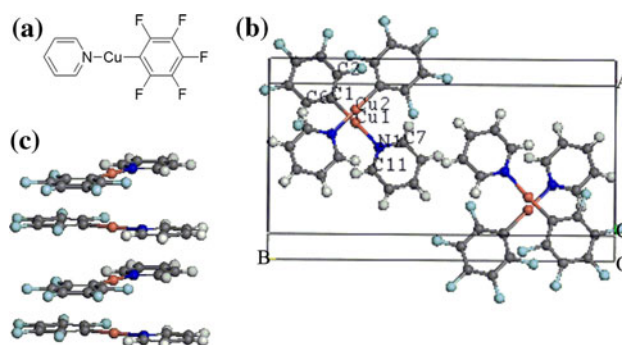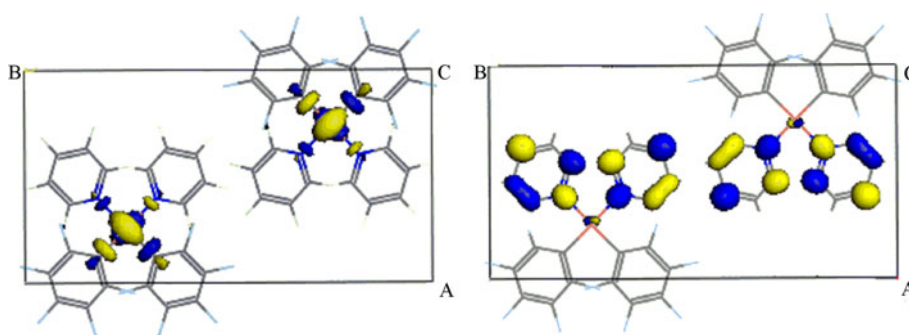

Fig. 1 a Chemical structure, b crystal structure, c packing mode along c-axis of $C_6F_5Cu(py)$

Table 1 Selected interatomic distances and angles of $C_6F_5Cu(py)$

Bond/angle	Cal	Exp
Distance (Å)		
Cu1–C1	1.875	1.891
Cu1–N1	1.893	1.902
Cu1–Cu2	2.894	2.892
Angle (°)		
C1–Cu1–N1	178.61	178.54
C7–N1–Cu1	121.84	121.11
C11–N1–Cu1	119.70	121.30
C6–C1–Cu1	120.57	121.80
C2–C1–Cu1	124.88	124.61
C1–Cu1–Cu2	88.89	89.90
N1–Cu1–Cu2	91.09	90.10

Fig. 2 Γ-point HOMO and LUMO wave functions for $C_6F_5Cu(py)$

centers of 2.80 Å [74], which leads to the presence of cuprophilic interactions, and such interactions may significantly influence the charge transport properties.

3.2 Analysis of frontier molecular orbitals

There is a close relationship between the charge transport and distribution of frontier molecular orbitals. The wave functions of the band-edge state at the Γ point are shown in Fig. 2, which are equivalent to the frontier molecular orbitals, namely, the HOMO for the hole and LUMO for the electron. Here, the yellow (blue) color is for positive (negative) wave functions values. As seen from the illustration, the wave functions of HOMO display a significant electronic density on the copper atoms while for LUMO mainly on pyridine groups. Thus, the hole is much more possibly transport along the direction of the cuprophilic interactions. Moreover, the close distances between two copper atoms along one-dimensional metal chains will also help to this transportation.

3.3 Band structure

The electronic band structure along high symmetry directions and corresponding density of states (DOS) are depicted in Figs. 3 and 4, respectively. From Fig. 3, we can see that both occupied and unoccupied bands consist of two subbands due to the two translationally inequivalent molecules present in the unit cell. $C_6F_5Cu(py)$ is an indirect semiconductor with a band gap of 1.31 eV with its maximum of valence band at Γ point and minimum of conduction band at X point. Furthermore, from the bandwidths of valence band and conduction band along different directions listed in Table 2, the largest dispersions for both valence and conduction bands are observed along the symmetry line between Z and Γ, which corresponds to the c-axis direction in real space or the alignment of the copper atoms in one-dimensional chains. There are no apparent dispersions along other directions. The bandwidth of valence band along the Z–Γ direction is 1.08 eV, which is three times larger than that of the conduction band
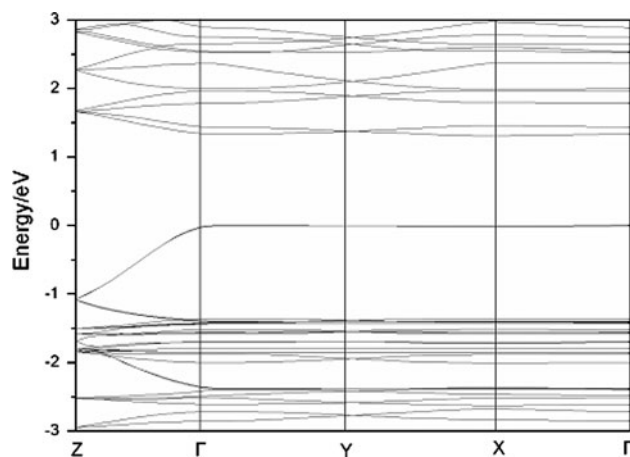

Fig. 3 Calculated band structure of $C_6F_5Cu(py)$ crystal. The high-symmetry points are $Z = (0,0,0.5)$, $\Gamma = (0,0,0)$, $Y = (0,0.5,0)$, $X = (0.5,0,0)$
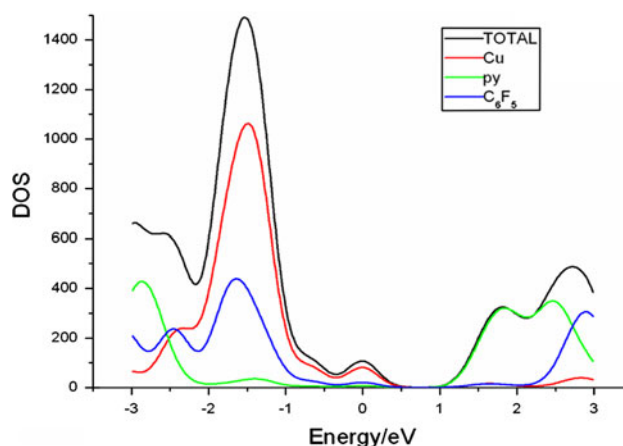

Fig. 4 Density of states (DOS) of $C_6F_5Cu(py)$ crystal

Table 2 Bandwidths of HOMO and LUMO along high symmetry directions in eV

	Z→Γ	Γ→Y	Y→X	X→Γ
LUMO	0.33	0.04	0.06	0.03
HOMO	1.08	0.01	0.00	0.01

Table 3 Effective masses m (in units of the electron mass at the rest, m_0) of electron and hole at the band edge in $C_6F_5Cu(py)$ crystal

	m/m_0
Electron	1.52
Hole	0.46

(0.33 eV). In general, the appearance of both dispersive and flat bands is a reflection of anisotropy in the charge transport properties of the crystal, and the stronger dispersion of band is, the larger carrier mobility is [75]. That is, the holes in valence band could move much easier than the electrons in conduction band. On the other hand, we can see clearly from density of states of the complex that copper atoms contribute significantly to the valence band, whereas to conduction band, pyridine group does, which is consistent with the analytic results of the frontier molecular orbitals. Thus, this indicates that the large dispersion of valence band and corresponding good hole transport abilities are all related to the interactions between copper atoms.

We further check the effective masses of the hole and electron. The mobility can be described using the effective mass approximation in the case of wide-band. In general, a smaller effective mass would lead to the easier carrier (electron or hole) transport. Based on the analysis of the band structure, there is no apparent dispersions along the directions except c-axis. Thus, the effective masses of both valence and conduction bands along c-axis using Eq. (3) were calculated, and their corresponding results are listed in Table 3. The effective mass for hole is 0.46 m_0, which is only one-third of the electron (1.52 m_0). From a band picture point of view, the inverse of effective mass is proportional to the mobility, thus indicating that the hole mobility should be 3 times larger than that of the electron. Moreover, the hole effective mass of $C_6F_5Cu(py)$ is much smaller than that of the pentacene (1.70 m_0), which is a typical hole transport material [76]. It is concluded that $C_6F_5Cu(py)$ is a good hole transport material. As mentioned earlier, such good transport ability is contributed to the copper–copper interactions.

3.4 Charge transport ability vs. metallophilic interactions

It is well known that tiny modification on structures or substitution can substantially improve their charge transport properties and mechanical processability [77–80]. Since the transport ability here is sensitive to the so called cuprophilic interactions, and such metallophilic interactions are related to relativistic effects [81, 82], we make an analysis on the relationship between the transport ability

Table 4 Selected interatomic distances and angles for $C_6F_5M(py)$ systems (M = Ag or Au)

	Ag	Au
Distance (Å)		
M1–C1	2.137	2.202
M1–N1	2.197	2.269
M1–M2	2.903	2.911
Angle (°)		
C1–M1–N1	176.16	175.96
C7–N1–M1	121.19	121.45
C11–N1–M1	119.87	119.37
C6–C1–M1	119.63	119.99
C2–C1–M1	123.96	123.38
C1–M1–M2	86.59	85.49
N1–M1–M2	93.18	94.18

Table 5 Calculated bandwidths of LUMO and HOMO along Z→Γ and binding energies (E) for $C_6F_5M(py)$ systems

	Cu	Ag	Au
LUMO (eV)	0.33	0.22	0.20
HOMO (eV)	1.08	1.26	1.57
E (kcal/mol)	−7.12	−9.13	−10.50

and metallophilic interactions. By replacing the copper atoms into silver and gold, we optimized the geometry structures and calculated the band structures of Ag and Au systems in Dmol^3 package with the same accuracy in Cu system. And the binding energies of pair molecules extracted from the optimized structures along c-axis are also calculated in Gaussian 09 program package. Table 4 presents the optimized bond lengths and angles of $C_6F_5M(py)$, where M denotes the Ag and Au atoms, and the labels here are consistent with that in Table 1. As increasing the metal atomic weights, the distance between metal atom and ligands are larger, but the angles of C1–M1–N1 are reduced from 178.61° (Cu) to 176.16° (Ag) and to 175.96° (Au), which leads to nonlinear conformation of the whole molecule, and the metal atoms along the c-axis are slightly staggered.

From the bandwidths and binding energies in Table 5, we can see that by enhancing the relativistic effects, the valence dispersions along c-axis are larger, whereas the conduction dispersions are smaller, which makes the holes transport much easier. On the other hand, the binding energies are larger with the displacement of metal atom from copper to gold. The value for Cu here (−7.12 kcal/mol) is larger than what we found in ref [82] of −4 kcal/mol. This means that the systems containing silver and gold will be more stable and exhibit more excellent hole transport ability. The calculated results also demonstrated

that metallophilic interactions contribute predominantly to the carrier transport abilities for $C_6F_5M(py)$.

3.5 Luminescent properties

As reported by Jakle et al., the crystal of $C_6F_5Cu(py)$ shows a strong blue fluorescence emission at $\lambda_{max} = 460$ nm in the solid state, we analyzed the luminescent properties by calculating the fluorescence spectrum. We optimized the ground state (S_0) and excited state (S_1) of the monomer and calculated the emission spectrum using TDDFT module within Gaussian 09 program. And we also calculated the dimer emission spectrum. However, due to the weak interactions between copper atoms, it is difficult to optimize the geometry structure of the dimer. We built the dimer by replacing each of the molecules in the dimer with the optimized S1 monomer. It has been demonstrated that this is an appropriate way to build dimer excited state geometry, and the results are in agreement with the experimental data [83]. To obtain more reliable results, we also employed other ways to analyze the luminescent properties of the dimer by constraining the geometry of single molecule, we optimized the distances of ground- and excited states between the two monomer molecules. The emission peak of monomer is 448.59 nm, which is close to the experimental value 460 nm, shown in Fig. 5. The dimeric results obtained from the two methods are similar, the emission peak of the former is 552.70 nm, and the latter is 543.08 nm, but there is about 90 nm difference compared with the experimental value. And the distance (2.851 Å) between two copper atoms in the excited state is shorter than that (2.919 Å) of the ground state. It should be noted that the metallophilic interactions possibly influence the emission [42, 84–87]. So, we further analyzed the relationship between the weak interaction and the emission by changing the distance of two molecules from 2.81 Å to 3.80 Å based on the optimized equilibrium distance (2.85 Å). In general, the distance of the cuprophilic interactions is between 2.5 Å and 3.5 Å [82]. The calculated results are shown in Table S1 (Supporting Information), and we can see the emission peak is redshift when the distance of two molecules is getting shorter than the optimized equilibrium distance, but when the distance of two molecules is getting larger, the emission peak is blueshift as shown in Figure S1, i.e., weakening the interaction between copper atoms makes

the emission peak closer to the emission of the monomer. Based on the above analysis, the solid state emission of $C_6F_5Cu(py)$ is attributed to the monomer rather than the dimer containing the weak interaction. This emission corresponds to the promotion of one electron from HOMO-2 to LUMO (Fig. 5), assigned as the metal-to-ligand charge transfer (MLCT), and combined with some contributions from ligand-to-ligand charge transfer (LLCT).

4 Conclusions

In summary, we investigated the electronic, luminescent, and charge transport properties of $C_6F_5Cu(py)$ through DFT and first-principle band-structure calculations. The results of band structure show a one-dimensional charge transport along c-axis, with a valence band dispersion of 1.08 eV, which is three times larger of the conduction band. Furthermore, the calculated effective mass for hole is only 0.46 m_0, which is only one-third of electron and much smaller than that of the pentacene. As a consequence, $C_6F_5Cu(py)$ has the potential to act as good hole transport material. The analysis based on density of states and band structure shows that hole transport are mainly along the direction of cuprophilic interactions and cuprophilic interactions are in favor of this transport. Replacement of copper atom with silver and gold, the results show that there is a close relationship between the metallophilic interactions and transport ability, i.e., the stronger metallophilic interactions are, the better hole transport property is. Thus, the systems containing silver and gold will be more stable and exhibit more excellent hole transport properties. The solid state emission of $C_6F_5Cu(py)$ is attributed to the monomer rather than the dimer. This emission is assigned as the metal-to-ligand charge transfer (MLCT) and combined with some contributions from ligand-to-ligand charge transfer (LLCT).

Fig. 5 Calculated singlet electron transition for monomer

References

1. Coropceanu V, Cornil J, da Silva Filho DA, Olivier Y, Silbey R, Brédas JL (2007) Chem Rev 107:926. doi:10.1021/cr050140x

2. Forrest SR, Thompson ME (2007) Chem Rev 107:923. doi:10.1021/cr0501590

3. Shirota Y, Kageyama H (2007) Chem Rev 107:953. doi:10.1021/cr050143+

4. Tang CW, VanSlyke SA (1987) Appl Phys Lett 51:913. doi:10.1063/1.98799

5. Baldo MA, O'Brien DF, You Y, Shoustikov A, Sibley S, Thompson ME, Forrest SR (1998) Nature 395:151. doi:10.1038/25954

6. Garnier F, Hajlaoui R, Yassar A, Srivastava P (1994) Science 265:1684. doi:10.1126/science.265.5179.1684

7. Sirringhaus H, Brown PJ, Friend RH, Nielsen MM, Bechgaard K, Langeveld-Voss BMW, Spiering AJH, Janssen RAJ, Meijer EW, Herwig P, de Leeuw DM (1999) Nature 401:685. doi:10.1038/44359

8. Sariciftci NS, Smilowitz L, Heeger AJ, Wudl F (1992) Science 258:1474. doi:10.1126/science.258.5087.1474

9. Halls JJM, Walsh CA, Greenham NC, Marseglia EA, Friend RH, Moratti SC, Holmes AB (1995) Nature 376:498. doi:10.1038/376498a0

10. Ford PC, Vogler A (1993) Acc Chem Res 26:220. doi:10.1021/ar00028a013

11. Ford PC, Cariati E, Bourassa J (1999) Chem Rev 99:3625. doi:10.1021/cr960109i

12. Kutal C (1990) Coord Chem Rev 99:213. doi:10.1016/0010-8545(90)80064-z

13. Ziessel R, Hissler M, El-ghayoury A, Harriman A (1998) Coord Chem Rev 178:1251. doi:10.1016/s0010-8545(98)00060-5

14. Chan CW, Cheng LK, Che CM (1994) Coord Chem Rev 132:87. doi:10.1016/0010-8545(94)80027-8

15. Roundhill DM, Gray HB, Che CM (1989) Acc Chem Res 22:55. doi:10.1021/ar00158a002

16. Fleeman WL, Connick WB (2002) Comments Inorg Chem 23:205. doi:10.1080/02603590212096

17. Mansour MA, Connick WB, Lachicotte RJ, Gysling HJ, Eisenberg R (1998) J Am Chem Soc 120:1329. doi:10.1021/ja973216i

18. Lee YA, McGarrah JE, Lachicotte RJ, Eisenberg R (2002) J Am Chem Soc 124:10662. doi:10.1021/ja0267876

19. Schmidbaur H, Cronje S, Djordjevic B, Schuster O (2005) Chem Phys 311:151. doi:10.1016/j.chemphys.2004.09.023

20. Fackler JP (2002) Inorg Chem 41:6959. doi:10.1021/ic025734m

21. Rawashdeh-Omary MA, Omary MA, Patterson HH, Fackler JP (2001) J Am Chem Soc 123:11237. doi:10.1021/ja011176j

22. Fernandez EJ, Lopez-de-Luzuriaga JM, Monge M, Rodriguez MA, Crespo O, Gimeno MC, Laguna A, Jones PG (1998) Inorg Chem 37:6002. doi:10.1021/ic980786q

23. Pan QJ, Zhou X, Fu HG, Zhang HX (2008) Organometallics 27:2474. doi:10.1021/om701114z

24. Pan QJ, Zhang HX (2003) Inorg Chem 43:593. doi:10.1021/ic0300159

25. Pan QJ, Zhou X, Guo YR, Fu HG, Zhang HX (2009) Inorg Chem 48:2844. doi:10.1021/ic801687w

26. Lu W, Chen Y, Roy VAL, Chui Stephen SY, Che CM (2009) Angew Chem 121:7757. doi:10.1002/ange.200903109

27. Chen Y, Li K, Lu W, Chui Stephen SY, Ma CW, Che CM (2009) Angew Chem Int Ed 48:9909. doi:10.1002/anie.200905678

28. Pyykko P (1997) Chem Rev 97:597. doi:10.1021/cr940396v

29. Pyykkö P, Straka M (2000) Phys Chem Chem Phys 2:2489. doi:10.1039/b001171l

30. Johnson AL, Willcocks AM, Richards SP (2009) Inorg Chem 48:8613. doi:10.1021/ic901051f

31. Che CM, Lai SW (2005) Coord Chem Rev 249:1296. doi:10.1016/j.ccr.2004.11.026

32. Leung KH, Phillips DL, Tse M-C, Che C-M, Miskowski VM (1999) J Am Chem Soc 121:4799. doi:10.1021/ja990195e

33. Fu WF, Chan KC, Miskowski VM, Che CM (1999) Angew Chem Int Ed 38:2783. doi:10.1002/(SICI)1521-3773(19990917)38:18<2783:AID-ANIE2783>3.0.CO;2-I

34. King C, Wang JC, Khan MNI, Fackler JP (1989) Inorg Chem 28:2145. doi:10.1021/ic00310a026

35. Che CM, Tse MC, Chan MCW, Cheung KK, Phillips DL, Leung KH (2000) J Am Chem Soc 122:2464. doi:10.1021/ja9904890

36. Che CM, Mao Z, Miskowski Vincent M, Tse MC, Chan CK, Cheung KK, Phillips David L, Leung KH (2000) Angew Chem 39:4084. doi:10.1002/1521-3773(20001117)39:22<4084:AID-ANIE4084>3.0.CO;2-N

37. Pyykkö P (2004) Angew Chem Int Ed 43:4412. doi:10.1002/anie.200300624

38. Pyykkö P, Li J, Runeberg N (1994) Chem Phys Lett 218:133. doi:10.1016/0009-2614(93)e1447-o

39. Narayanaswamy R, Young MA, Parkhurst E, Ouellette M, Kerr ME, Ho DM, Elder RC, Bruce AE, Bruce MRM (1993) Inorg Chem 32:2506. doi:10.1021/ic00063a051

40. Vickery JC, Olmstead MM, Fung EY, Balch AL (1997) Angew Chem Int Ed 36:1179. doi:10.1002/anie.199711791

41. Cariati E, Bourassa J (1998) Chem Comm 1623. doi:10.1039/a802805b

42. Dias HVR, Diyabalanage HVK, Rawashdeh-Omary MA, Franzman MA, Omary MA (2003) J Am Chem Soc 125:12072. doi:10.1021/ja036736o

43. Ma Y, Chao H-Y, Wu Y, Lee ST, Yu WY, Che CM (1998) Chem Comm 2491. doi:10.1039/a805236k

44. Rawashdeh-Omary MA, Omary MA, Shankle GE, Patterson HH (2000) J Phys Chem B 104:6143. doi:10.1021/jp000563x

45. Grimes T, Omary MA, Dias HVR, Cundari TR (2006) J Phys Chem A 110:5823. doi:10.1021/jp0605146

46. Slyke SAV, Chen CH, Tang CW (1996) Appl Phys Lett 69:2160. doi:10.1063/1.117151

47. Yu B, Zhu F, Wang H, Li G, Yan D (2008) J Appl Phys 104:114503. doi:10.1063/1.3033485

48. Jäkle F (2007) Dalton Trans 2851. doi:10.1039/b704372d

49. Doshi A, Venkatasubbaiah K, Rheingold AL, Jäkle F (2008) Chem Comm 4264. doi:10.1039/b807128d

50. Sundararaman A, Zakharov LN, Rheingold AL, Jäkle F (2005) Chem Comm 1708. doi:10.1039/b417532h

51. Delgado MCR, Pigg KR, da Silva Filho DTA, Gruhn NE, Sakamoto Y, Suzuki T, Osuna RM, Casado J, Hernández Vc, Navarrete JTLP, Martinelli NG, Cornil J, Sánchez-Carrera RS, Coropceanu V, Brédas JL (2009) J Am Chem Soc 131:1502. doi:10.1021/ja807528w

52. Salman S, Delgado MCR, Coropceanu V, Brédas JL (2009) Chem Mater 21:3593. doi:10.1021/cm901128j

53. Long M, Tang L, Wang D, Wang L, Shuai Z (2009) J Am Chem Soc 131:17728. doi:10.1021/ja907528a

54. Calzolari A, Alexandre SS, Zamora F, Di Felice R (2008) J Am Chem Soc 130:5552. doi:10.1021/ja800358c

55. Gao H, Qin C, Zhang H, Wu S, Su ZM, Wang Y (2008) J Phys Chem A 112:9097. doi:10.1021/jp804308e

56. Yang GC, Liao Y, Su ZM, Zhang HY, Wang Y (2006) J Phys Chem A 110:8758. doi:10.1021/jp061286i

57. Wu J, Wu S, Geng Y, Yang G, Muhammad S, Jin J, Liao Y, Su Z (2010) Theo Chem Acc 10.1007/s00214. doi:10.1007/s00214-010-0730-x

58. Yang Y, Geng H, Yin S, Shuai Z, Peng J (2006) J Phys Chem B 110:3180. doi:10.1021/jp0540252

59. Yang CH, Su WL, Fang KH, Wang SP, Sun IW (2006) Organometallics 25:4514. doi:10.1021/om060323p

60. Liu T, Zhang HX, Xia BH (2007) J Phys Chem A 111:8724. doi:10.1021/jp072802n

61. Delley B (1990) J Chem Phys 92:508. doi:10.1063/1.458452

62. Delley B (2000) J Chem Phys 113:7756. doi:10.1063/1.1316015

63. Byrd EFC, Scuseria GE, Chabalowski CF (2004) J Phys Chem B 108:13100. doi:10.1021/jp0486797

64. Perdew JP, Burke K, Ernzerhof M (1996) Phys Rev Lett 77:3865. doi:10.1103/PhysRevLett.77.3865

65. Head-Gordon M, Pople JA, Frisch MJ (1988) Chem Phys Lett 153:503. doi:10.1016/0009-2614(88)85250-3

66. Frisch MJ, Trucks GW, Schlegel HB, Scuseria GE, Robb MA, Cheeseman JR, Scalmani G, Barone V, Mennucci B, Petersson GA, Nakatsuji H, Caricato M, Li X, Hratchian HP, Izmaylov AF, Bloino J, Zheng G, Sonnenberg JL, Hada M, Ehara M, Toyota K, Fukuda R, Hasegawa J, Ishida M, Nakajima T, Honda Y, Kitao O, Nakai H, Vreven T, Montgomery JJA, Peralta JE, Ogliaro F, Bearpark M, Heyd JJ, Brothers E, Kudin KN, Staroverov VN, Kobayashi R, Normand J, Raghavachari K, Rendell A, Burant JC, Iyengar SS, Tomasi J, Cossi M, Rega N, Millam JM, Klene M, Knox JE, Cross JB, Bakken V, Adamo C, Jaramillo J, Gomperts R, Stratmann RE, Yazyev O, Austin AJ, Cammi R, Pomelli C, Ochterski JW, Martin RL, Morokuma K, Zakrzewski VG, Voth GA, Salvador P, Dannenberg JJ, Dapprich S, Daniels AD, Farkas O, Foresman JB, Ortiz JV, Cioslowski J, Fox GDJ (2009) Gaussian 09, Revision A.02, Gaussian, Inc., Wallingford, CT

67. Becke AD (1993) J Chem Phys 98:5648. doi:10.1063/1.464913

68. Lee C, Yang W, Parr RG (1988) Phys Rev B 37:785. doi:10.1103/PhysRevB.37.785

69. Özen C, Tüzün NS (2008) Organometallics 27:4600. doi:10.1021/om800094k

70. Geisberger G, Klapötke TM, Stierstorfer J (2007) Eur J Inorg Chem 2007:4743. doi:10.1002/ejic.200700395

71. Ditchfield R, Hehre WJ, Pople JA (1971) J Chem Phys 54:724. doi:10.1063/1.1674902

72. Gordon MS (1980) Chem Phys Lett 76:163. doi:10.1016/0009-2614(80)80628-2

73. Boys SF, Bernardi F (1970) Mol Phys 19:553. doi:10.1080/00268977000101561

74. Bondi A (1964) J Phys Chem 68:441. doi:10.1021/j100785a001

75. Delgado MCR, Kim E-G, Filho DtAdS, Brédas JL (2010) J Am Chem Soc 132:3375. doi:10.1021/ja908173x

76. de Wijs GA, Mattheus CC, de Groot RA, Palstra TTM (2003) Synth Met 139:109. doi:10.1016/s0379-6779(03)00020-1

77. Sirringhaus H, Wilson RJ, Friend RH, Inbasekaran M, Wu W, Woo EP, Grell M, Bradley DDC (2000) Appl Phys Lett 77:406. doi:10.1063/1.126991

78. Shimizu Y, Oikawa K, Nakayama KI, Guillon D (2007) J Mater Chem 17:4223. doi:10.1039/b705534j

79. Adam D, Schuhmacher P, Simmerer J, Haussling L, Siemensmeyer K, Etzbachi KH, Ringsdorf H, Haarer D (1994) Nature 371:141. doi:10.1038/371141a0

80. Kim E-G, Brédas JL (2008) J Am Chem Soc 130:16880. doi:10.1021/ja806389b

81. Pyykkö P, Runeberg N, Mendizabal F (1997) Chem Eur J 3:1451. doi:10.1002/chem.19970030911

82. Hermann HL, Boche G, Schwerdtfeger P (2001) Chem Eur J 7:5333. doi:10.1002/1521-3765(20011217)7:24<5333:AID-CHEM5333>3.0.CO;2-1

83. Hu B, Gahungu G, Zhang J (2007) J Phys Chem A 111:4965. doi:10.1021/jp0689215

84. Lee YA, Eisenberg R (2003) J Am Chem Soc 125:7778. doi:10.1021/ja034560k

85. White-Morris RL, Olmstead MM, Balch AL (2003) J Am Chem Soc 125:1033. doi:10.1021/ja020902v

86. Hayashi A, Olmstead MM, Attar S, Balch AL (2002) J Am Chem Soc 124:5791. doi:10.1021/ja012416y

87. Fernández EJ, Gimeno MC, Laguna A, López-de-Luzuriaga JM, Monge M, Pyykkö P, Sundholm D (2000) J Am Chem Soc 122:7287. doi:10.1021/ja9942540